한국부식학회지
J. Corros. Sci. Soc. of Korea
Vol. 18 No. 3 Sept, 1989
〈研究論文〉

Plasma-Sprayed Alumina-Yttria Ceramic Coatings for Cavitation-Erosion Protection

Hee Jae Kim

Department of Ordnance Engineering
Korea Military Academy

A series of alumina-yttria composite powders were plasma-sprayed on the carbon steel plate. The microstructures of sprayed coating layers were characterized, and their cavitation-erosion resistance were examined.

It was found that alumina-yttria composite powder coatings produced a large grained equi-axed structure of alumina phases, with very fine elongated yttria precipitates as well as yttria-alumina garnet phases. Alumina coatings with 3 - 5 wt. % yttria additions significantly increased the hardness and resistance to cavitation-erosion environment.

1. INTRODUCTION

Plasma-sprayed ceramic coatings are extensively used in several applications to protect critical components from severe environmental conditions. The ceramic coatings offer several attractive properties, such as high hardness[1], wear and erosion resistance[2-3], corrosion resistance[4], and the change in the electrical property[5].

A ceramic of interest in the point of corrosion and erosion resistance is alumina[3]. One problem, however, with alumina is the introduction of intergranular cracks and fissures which are atrributed to thermal shock and to the substantial difference in thermal contraction or expansion between coating and substrate[6]. Furthermore, cracks and voids are produced due to the convergence of phase transformation from the metastable γ-alumina to the stable α-alumina, when the alumina coatings were exposed to the temperature above 1000°C.[7]

Titania can be frequently added to prevent this reversion in alumina coatings as a flux[8]. Wilms[6] studied the effects of yttria addition in the range of 3 - 20 wt. % to alumina on the microstructure of the plasma-sprayed alloyed coatings. He found that yttria addition to alumina resulted in a more rigid-joined interface and a more uniformly filled coating.

In this present work, the effects of yttria addition to the alumina coatings on both microstructural change and cavitation-erosion behavior were studied. Experiments were conducted to

Table 1. Chemical Composition of As-received Powders (wt. %)

Powder	Al_2O_3	Y_2O_3	SiO_2	Fe_2O_3	CaO	NaO	Others
Alumina	99.8		0.03	0.01		0.13	0.03
Yttria	0.02	99.9	0.009	0.02	0.002		0.049

examine the microstructure of plasma-sprayed coatings using scanning electron microscopy (SEM), transmission electron microscopy (TEM), x-ray diffraction, and microprobe analysis, and to evaluate their cavitation-erosion resistance.

2. EXPERIMENTAL PROCEDURES

The powders selected for the deposition of the coatings were commercially obtained, supplied by Japan Abrasive Co., Ltd.. The specification of the as-received powders is illustrated in Tables 1 and 2. Alumina-yttria composite powders (alumina - 1, 2, 3, 5, and 10 wt. % yttria) were made by mechanical mixing of alumina and yttria powders for approximately 6 hours in a jar mill.

Table 2. Particle Size Distribution of As-received Powder

	Size(μm)	Mean Diameter(μm)
Alumina	$-60+15$	22
Yttria	$-52+7$	21

Plasma spraying was carried out energizing by 32.5 KW with a METCO HP-3MB gun system in the air with argon/hydrogen mixture for the plasma forming gas, according to the spraying parameters given in Table 3. Cold-rolled SAE C1080 steel was used for spraying substrates in the form of plate (1 cm x 7.5 cm x 0.3 cm). The applied coatings were approximately 0.025 cm in thickness.

Table 3. Plasma Spray Parameters

Current (A)	500
Voltage (V)	65
Argon Flow (Standard ft^3/min) Primary Gas	80
Hydrogen Flow (Standard ft^3/min) Secondary Gas	15
Powder Feed Gas Flow (METCO powder feed rate)	40
Powder Feed Rate (ℓb/min)	3.2
Spray Distance (㎝)	63.5

X-ray diffractometry was carried out using monochromatized Cu K_α radiation generated at 45 KV and 40 amp. to analyze the phases present in the powders and their coatings.

A scanning electron microscopy was used to examine the gold sputtered as-sprayed coatings. Porosity of the coatings was measured by image analysis of the SEM photos. Microprobe analysis was conducted on the cross-sectional area of the coatings using an accelerating voltage of 15 KV and current of 30 mA to obtain the chemical composition of the observed phases.

Transmission electron microscopy (Philips, operated at 200 KV) was also conducted to examine the microstructure of the coating layers.

Both the microhardness (diamond pyramid hardness at a load of 300 g_f) and superficial

Rockwell hardness (load, 15 Kg_f; diamond "N" brale) were measured.

An ultrasonic vibratory cavitation apparatus supplied by Branson Sonic Power Co. was used for conducting the cavitation-erosion tests. The amplitude of vibration was maintained constantly at 40 μm through the test using an ultrasonic vibrator at frequency of 20 kHz in the distilled water. The tests were carried out in accordance with ASTM G32-77 with the 0.0635 cm distance. All specimens were tested in the as-sprayed condition without further surface treatment. Weight loss was measured as a function of exposure time to evaluate the cavitation-erosion resistance of each coating.

3. RESULTS AND DISCUSSION

Microstructural Analysis of coatings.

Fig. 1 shows the cross-sectional SEM microstructure of the sprayed coatings. As shown in the figures, sprayed coating layers are porous. The porosity was slightly reduced as increasing

(a) alumina

(b) alumina-3 wt.% yttria

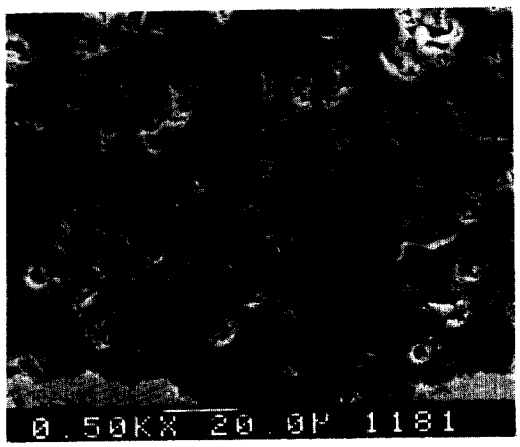

(c) alumina-5 wt.% yttria

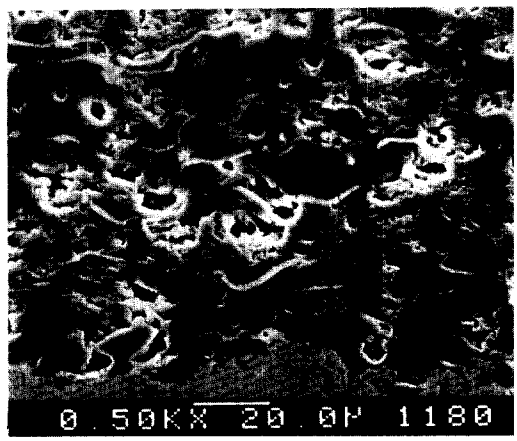

(d) alumina-10 wt.% yttria

Fig. 1 Cross-sectional SEM micrographs of plasma-sprayed coatings

the yttria addition to alumina as illustrated in Table 4. However, alumina-10 wt. % yttria coating showed the highest porosity in the present study. The size, volume fraction and distribution of pores in the sprayed coating can influence both strength and permeability and, hence, are important factors in determining protective qualities.

Table 4. Porosity of the Plasma-sprayed Layer

Material	Average Porosity (Volume%)
Al_2O_3	14.3
Al_2O_3 – 1 wt.% Y_2O_3	13.1
Al_2O_3 – 2 wt.% Y_2O_3	12.3
Al_2O_3 – 3 wt.% Y_2O_3	11.8
Al_2O_3 – 5 wt.% Y_2O_3	9.7
Al_2O_3 – 10 wt.% Y_2O_3	17.5

Table 5 shows the phase present in the powders and coatings. As-sprayed composite coatings consist principally of metastable γ-alumina phase with small amounts of equilibrium α-Al_2O_3 and Y_2O_3 phases. The x-ray intensities of Y_2O_3 phase in the composite coatings are increased as the weight percent ratio of Y_2O_3 to Al_2O_3 is increased.

Fig. 2 shows the x-ray diffraction of alumina

Table 5. Phase Present in Powders and Their Plasma-sprayed Coatings

Material	Powder Phases	Coating Phases
Al_2O_3	$\alpha - Al_2O_3$(Corundum)	$\underline{\gamma} - Al_2O_3 + \alpha - Al_2O_3$
$AlO - x$ wt.% Y_2O_3 $x = 1, 2, 3, 5, 10$	$\underline{\alpha} - Al_2O_3 + Y_2O_3$	$\underline{\gamma} - Al_2O_3 + \alpha - Al_2O_3 + Y_2O_3 + 1/2(3Y_2O_3 \cdot 5Al_2O_3)$

(Note) Underline – major phase

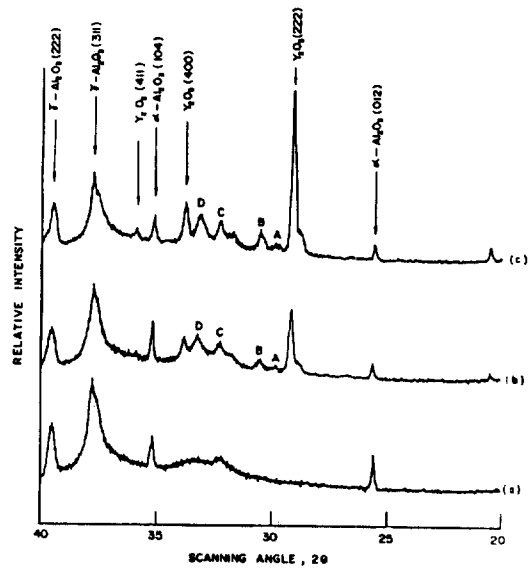

Fig. 2 X-ray diffraction of as-sprayed coatings : (a) alumina, (b) alumina-5 wt.% yttria, and (c) alumina-10 wt.% yttria.

and alumina - 5 and 10 wt. % yttria coatings. Sharp α-Al_2O_3 peaks in Fig. 2(a) indicate incomplete melting of sprayed powders. Peak broadening between 32.0 - 34.0° in the x-ray scattering angle, which could not be identified by JPS cards, seems to indicate that an amorphous or very fine grained phase is present. In the diffraction of alumina - 5 wt. % yttria coating(Fig. 2(b)), cubic Y_2O_3 peaks were observed. Some sharp Y_2O_3 peak also indicates the incomplete melting of the yttria powder. Their intensities are more pronounced in the alumina - 10 wt. % yttria coating. Four new peaks which were not detected in the pure alumina coatings were observed in the composite coatings at around 29.5 - 34° as marked with A, B, C, D in Fig. 2(b). The new peaks could be identified with yttrogarnet phases (that is, A: $2Y_2O_3.Al_2O_3$, B: $3Y_2O_3.5Al_2O_3$,

C: $YAlO_3$, D: $3Y_2O_3.5Al_2O_3$). All observation in the alumina - 10 wt. % yttria coating are similar to those in the alumina - 5 wt.% yttria coating. However, those new peaks are more intense.

Alumina-yttria composite coatings are composed of three regions, as shown in Fig. 3, with the contrast of white(marked P), light gray(marked G), and dark gray(matrix). According to the electron back scattering analysis of the coatings, white and dark gray regions were turned out to be Y_2O_3 and Al_2O_3 phase, respectively. Components in the range of approximately 7.27 to 35.25 wt. % Y_2O_3 existed in the light gray region were confirmed to be yttrogarnet structure, as previously found in the x-ray diffraction. In terms of the x-ray and microprobe analyses, the mechanical mixtures mostly splat and resolidify independently during spraying. However, it is possible for two or more splats to hit the substrate at the same time and to solidify together forming an alloy such as yttrogarnet in the range of composition to exist. The probability of this event occurrence increases with increasing the amount of yttria added.

(a) alumina-5 wt.% yttria

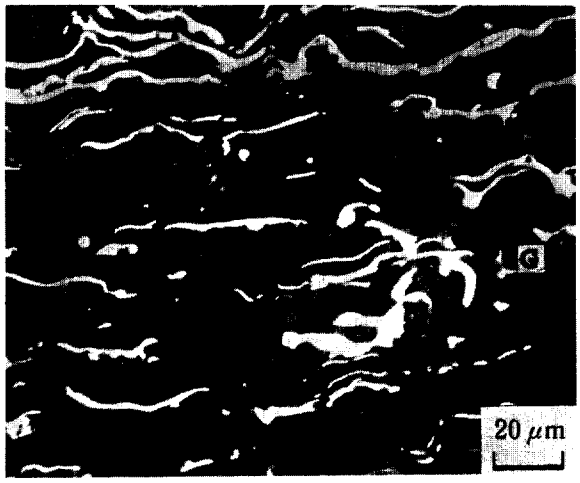

(b) alumina-10 wt.% yttria

Fig. 3 Electron back scattering of cross-sections of plasma-sprayed coatings.

The density of platelets was increased as increasing yttria adding to the alumina as shown in Fig. 3. The pores are observed in the overall coating layer. However, they are not much observed in-between the individual lamellar precipitates. This is likely due to the yttria-rich phases which were solidified at a temperature above the alumina melting temperature(2305 K). These yttria precipitates are, therefore, able to flow more easily, enabling a more complete interaction with the alumina, and filling the alumina in the interstices between the more rigid yttria platelets. In the alumina - 10 wt. % yttria, however, the pores are produced between the Y_2O_3 precipitates which are in a small distance. It seems to be a tolerable distance between the precipitates, which can be flowed very easily, to fill the alumina between rigid Y_2O_3 precipitates.

(a) crystalline alumina matrix

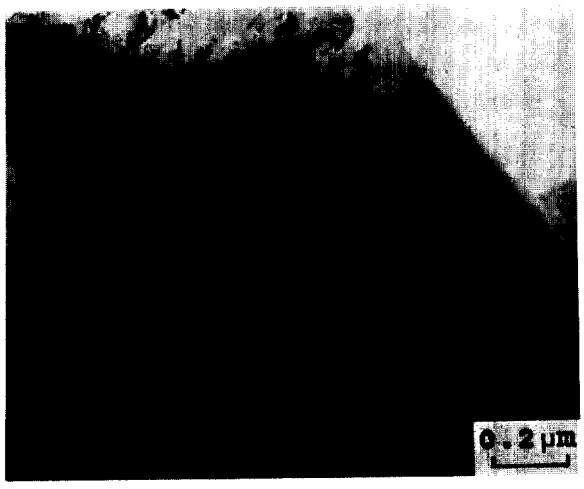

(b) a Y_2O_3 precipitate

Fig. 4 Transmission electron micrographs of plasma-sprayed alumina-5 wt.% yttria composite coatings

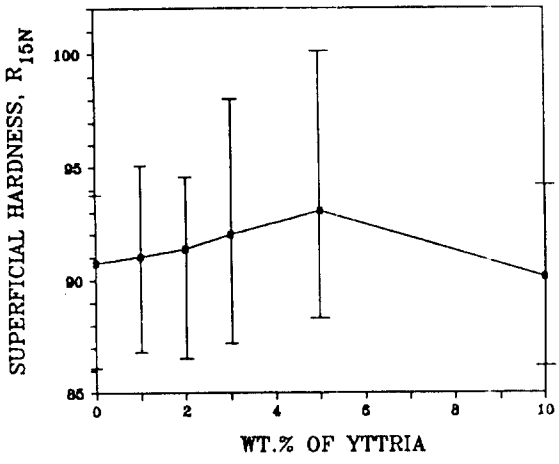

(a) superficial Rockwell hardness

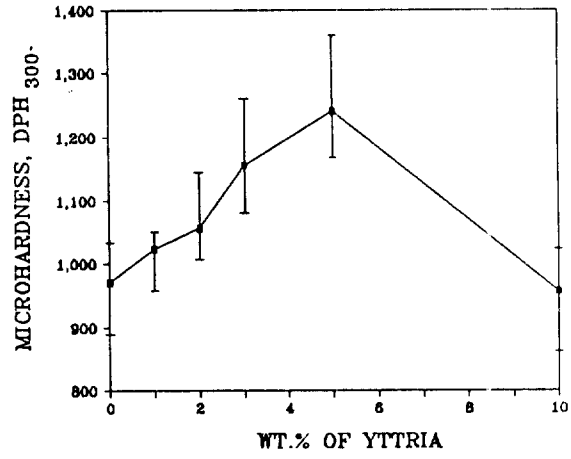

(b) diamond pyramid microhardness

Fig. 5 Hardness of plasma-sprayed alumina-yttria composite coatings.

Fig. 4 shows the TEM microstructures of plasma-sprayed alumina-yttria composite coatings. The overall microstructure of the coatings consisted of two phases which are equiaxed crystalline alumina matrix(0.5 - 2 μm in grain size) (Fig. 4(a)) and very fine yttria-rich precipitates(Fig. 4(b)). The precipitate shows the flattened platelets, which contain fine grained columnar grains. No difference in the microstructure between alumina - 5 and 10 wt. % yttria composite coatings was observed.

Cavitation-Erosion Behavior of Coatings

Fig. 5 shows both the superficial Rockwell hardness and cross-sectional microhardness of the

composite coatings. Both hardness are increased as increasing the addition of yttria to alumina. However, in the alumina - 10 wt. % yttria composite, a dramatic decrease in both hardness can be seen. The increase in hardness with adding yttria to alumina in the range of 1 - 5 wt. % may be attributed to the reduction of porosity and the presence of yttria and yttria-garnet structural precipitates in the coatings. Otherwise, the decrease in the hardness in the alumina - 10 wt. % yttria composite is presumably due to the high porosity and the presence of a lots of yttria precipitates. As previously described before, furthermore, the large size of pores formed in-between Y_2O_3 precipitates might be also responsible for the lower hardness of the alumina - 10 wt. % yttria composite coating.

Fig. 6 shows the cavitation-erosion resistance of plasma-sprayed alumina-yttria composite coatings. As shown in this figure, high resistance to cavitation-erosion was observed in alumina - 3 or 5 wt. % yttria composite coatings. Alumina - 1 or 2 wt. % yttria coatings also showed better erosion resistance than that of alumina coatings until about 1 hour exposure. After this exposure, the erosion resistance was lowered compared to alumina coating. However, the lowest erosion resistance was observed in alumina - 10 wt. % yttria coatings in this present study.

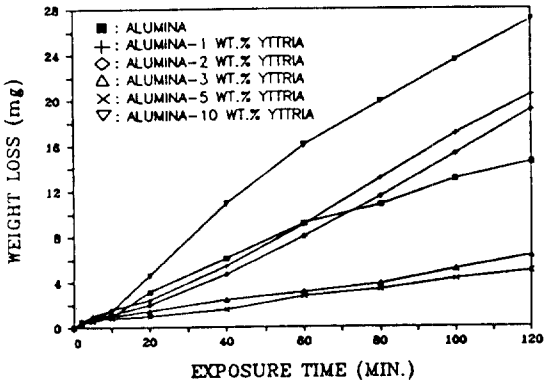

Fig. 6 Weight loss vs exposure time curves of plasma-sprayed alumina-yttria composite coatings.

The cavitation-erosion resistance is seemed to be associated with porosity, number of precipitates, hardness, and binder content. The erosion resistance of alumina-yttria composite coating is increased with reduced porosity, increased hardness and alumina binder content of yttria. However, if more yttria(10 wt. % yttria in the present study) is added, the resistance then decreased. The cause of this decrease in high yttria content composite coatings is likely due to high porosity and the formation of more yttria precipitates resulting in the reduction of binding effect in the coatings. It is not clear what causes the reduced erosion resistance of 1 or 2 wt. % yttria composite coating after about 1 hour exposure. The effect of each individual factor such as porosity and binder content on the cavitation-erosion resistance has remained unexplored.

All composite coatings have the similar surface roughness with R_a (arithmetic average) in the range of 3.5 - 6.5 μm AA. But a relatively fine surface in the alumina coatings was produced. It might be due to the unique particle size and melting temperature compared to the other composite powders. Thus surface topography may not influence on the cavitation-erosion testing.

4. CONCLUSIONS

1) Alumina phase produces a large grained structure while yttria forms a very fine grain

elongated to the direction of thermal extraction.

2) Plasma spraying of mechanically mixed alumina-yttria powder produces several types of yttria-alumina garnets during spraying resulting form the formation of an alloy when melt together.

3) Small quality(up to 5 wt. %) of mechanical mixing of yttria to alumina significantly increases the hardness of alumina coating.

4) Mechanical mixing of 5 wt. % yttria to alumina shows the excellent resistance to cavitation-erosion environment.

ACKNOWLEDGEMENT

The present study was supported by Korea Science and Engineering Foundation. The author is grateful to Prof. H. Herman and Dr. B. Gudmundsson, State University of New York at Stony Brook for their guidance.

REFERENCES

1. D. Chuanxian, R.A. Zatorski, and H. Herman, Thin Solid Films, **118** (1984) 467.
2. A. Levy and N. Jee, Wear, **121** (1988) 363.
3. A. Akhtar, Materials Performance, August (1982) 15.
4. H. Behnisch, Technica, **15** (1971) 1383.
5. I. Preece and C.W.D. Andrews, J. Mat. Sci., 8 (1973) 964.
6. V.H.S. Wilms: Microstructure of Plasma Sprayed Ceramic Coatings, *Ph.D. Thesis*, State University of New York at Stony Brook, NY(1978)
7. V.S. Thompson and O.J. Whittmore Jr., Am. Cer. Soc. Bull., 47 (1968) 637.
8. F. Eichhorn and J. Metzler, Metalloberflache 22 (1968) 225.